Title:

Late Fetal and Newborn Granulopoiesis but not Active Renin is Increased by Maternal Captopril Treatment During Perinatal Kidney Development

Authors:

[1]Buckley C*, [1]L'Huillier N*, [1]Mullins L, [1]Semprini S, [2]Christian H, [1]Mullins JJ

Affiliations:

[1]University/ BHF Centre for Cardiovascular Science, University of Edinburgh, Edinburgh EH16 4TJ, UK

[2]Department of Physiology, Anatomy and Genetics, University of Oxford, Oxford, UK

*Joint first authors

Corresponding Author:
Dr Linda J. Mullins
University/ BHF Centre for Cardiovascular Science
University of Edinburgh
47 Little France Crescent
Edinburgh
EH16 4TJ, UK
Tel: +44 (0)131-242-6722
Fax: +44 (0)131-242-6782
Linda.Mullins@ed.ac.uk

Abstract:

Renin expression follows vascular development through the mouse kidney, regressing to glomerular poles by about P10, where renin is stored in dense core granules in juxtaglomerular cells. Homeostatic challenge to blood pressure causes release of active renin from the granules and recruitment of the renin lineage cells. We investigated the response to homeostatic challenge during late fetal development and following birth in a transgenic line expressing GFP under the renin promotor. Pregnant females were treated with water or captopril (30mg/kg/day), which inhibits angiotensin converting enzyme, from E15.5. We found an increase in renin transcription and expression by P1 following captopril treatment, with granulation increased at the glomerular poles and major arteries from E18.5. At P1, the granules showed a wide variation in electron density. Notably, rough endoplasmic reticulum was expanded in vascular smooth muscle cells (VSMCs) of captopril-treated pups at both time-points suggesting increased transcriptional activity. Paracrystalline material was observed in granules of captopril treated fetuses at E18.5 and in both treated and untreated pups at P1. Renin expression and some granules were confirmed in the kidney VSMCs by immuno-gold staining against GFP at E18.5. Importantly, we found no difference in active renin content between kidneys from treated and untreated pups at either age group. We therefore demonstrate a disconnect between granulation and active renin production in newborns when exposed to homeostatic challenge *in utero*.

Introduction:

The renin-angiotensin system (RAS) is one of the key enzymatic cascades regulating blood pressure, water and electrolyte homeostasis. In addition to its endocrine function, roles relating to the innate immune system in disease states such as inflammation [1], pre-B cell leukemia [2] and fibrosis, [3,4] tissue repair [5] or regeneration and trans-differentiation following glomerular damage [6-9] have been identified. The transcription and expression of RAS components in multiple utero-placental cell types has also been reported in humans and mice [10]. Many of these extra-renal sites of expression may reflect local autocrine or paracrine actions of RAS.

Renin is an aspartyl protease, the function of which is to cleave its only known substrate, angiotensinogen, producing the decapeptide angiotensin (Ang) I by proteolytic cleavage at the N-terminus [11]. Renin is synthesized as a pre-pro-enzyme of 50kDa in humans [12] and mice [13]. In humans, the kidney is the only known organ to release active renin, whilst extra-renal sites secrete prorenin exclusively [14]. However, some renin-producing tumours have been described [15,16]. In addition, in the mouse, active renin has been found to be released by the submandibular gland [17] and by the adrenal gland [18].

Using antisera corresponding to the N-terminus, the C-terminus and the prosegment, Taugner *et al*. determined the fate of human prorenin during granule secretion [19]. Both in humans and mice, prorenin can be released constitutively[20], or packaged into low density protogranules that fuse and mature into dense core storage granules, as prorenin is converted to active renin (40kDa) for storage until controlled secretion is required [21]. It is here that the 43 amino acid NH_2 terminal pro-segment is cleaved off[20], though the manner in which this occurs is controversial. Candidate prohormone convertases have been shown to cleave renin *in vitro*, however mouse knockout models for these enzymes did not alter active renin *in vivo*. For instance, whilst cathepsin B was shown to co-localise with renin inside dense core granules and showed site-specific cleavage of the pro-segment *in vitro*[22], levels of active renin and prorenin remained the same in knockout mice as in controls[23,24]. There is evidence to suggest that after initial cleavage at the dibasic site, the pro-segment is slowly broken up until only the stable renin protein remains[25].

In the adult kidney, active renin is released from a population of cells of the juxtaglomerular apparatus, the juxtaglomerular (JG) cells [26]. JG cells are considered to be terminally differentiated from vascular smooth muscle cells (VSMC) since they possess VSMC characteristics and produce active renin. They derive from a pericyte lineage[27]; renin and pericyte markers such as αSMA and NG2 are coincidentally expressed during human kidney development, and primary cultures of pericytes isolated from human fetal kidney can be induced to express renin and form granules after stimulation with IBMX and forskolin[28] Although some renin-expressing cells are present prior to vessel formation in the loose renal mesenchyme [29], renin expression in the developing mouse kidney essentially follows the formation of the arcuate and interlobar arteries [30] beginning on day E14 [31]. As the renal artery divides further from interlobular arteries into arcuate arteries and afferent arterioles, renin expression follows this pattern and regresses in the larger arteries as the smaller arteries are formed, until it's expression is confined to the classic juxtaglomerular location at approximately P10 [31]. Sauter *et al* did not observe renin expression in the regions of greatest vascular growth and branching, suggesting that an established functional vessel wall is necessary for the onset of renin expression. However, the presence of renin during development suggests a physiological role of renin before blood pressure regulation commences.

In adults, when long term homeostasis is threatened, such as under chronic administration of angiotensin converting enzyme (ACE) inhibitors or low salt, vascular smooth muscle cells of the afferent arteriole, renal glomerular cells, mesangial cells and even interstitial cells are able to revert to a renin-producing phenotype[32]. This process, known as reversible metaplastic transformation[33] or plasticity[34], allows the production of renin in response to physiological challenges and is characterized by prorenin synthesis, granulopoiesis and the accumulation of mature granules to process prorenin into active renin. This pattern of recruited cells strongly resembles the ontogeny of renin development within the cortical vasculature[35].

Post-natally, the presence of renin granules is unequivocal [36,37]. However, few reports demonstrate the presence of renin granules in JG cells during renal development. In

the pig, two reports showed the presence of granules in the mesonephros and metanephros (precursors of the mature kidney) [37,38]. The presence of rare juxtamedullary juxtaglomerular renin granules was observed in Wistar rats at E18, with only occasional granules observed by E20 [36]. Minuth *et al*., reported the presence of renal renin granules in NMRI mice [39], though transmission electron microscopy data was not shown. In human foetuses, a juxtaglomerular index (the number of granules/number of cells) of zero or below one was recorded [40] but granules were identified in metanephric tissue[41].

It is, therefore, important to clarify whether renin dense core granules are present at the perinatal stage, and whether renin expression can be stimulated. We used transgenic animals expressing GFP under the renin promotor to show that ACE inhibition is a stimulus for renin transcription and perinatal granulopoiesis but is not a stimulus for storage of active renin.

Experimental Procedures:

Experiments were approved by the University of Edinburgh Animal Welfare and Ethical Review body (AWERB) and were conducted in accordance with the Animals (Scientific Procedures) Act 1986 and the Guiding Principles for Research Involving Animal.

Transgenic animals and ACE inhibition studies

RenGFP$^{+/-}$ mice[42], on a C57Bl6/J background, were used throughout the study. Females were paired with males in the afternoon and were examined for vaginal plugs the following morning. The time of plug detection was termed E0.5. Pregnant mice were housed individually, and either water (control group; n=7) or captopril (30mg/kg/day in water; treatment group; n=5) was administered via gavage. Due to reports of fetal toxicity during maternal exposure in rats[43], captopril (and water) gavage was started at E15.5. Male and female embryos were collected at E18.5 (n=5 water-treated mothers; n=2 captopril-treated mothers) and P1 (n=2 water-treated mothers; n=3 captopril-treated mothers) after CO_2 administration, and both sexes were used in the studies performed.

Genotyping

Tails were collected and digested overnight following manufacturer's instructions with DirectPCR lysis buffer (Viagen Biotech, 120-T). PCR was performed using VWR 2 mM $MgCl_2$ Red Taq DNA polymerase 2X mastermix, following manufacturer's instructions. Previously-published primers[44] were used to determine the sex of the pups.

Transmission Electron Microscopy

Ultrastructure Analysis

Embryonic and post-natal kidneys were cut in half and immersion fixed in 2.5% gluteraldehyde in 0.1M phosphate buffer (pH 7.2). Tissue was stored in this fixative for 4 hrs at room temperature, then transferred to a 10-fold dilution of buffer and stored at 4^{o}C before preparation for electron microscopy by standard methods [45]. Briefly, cells were post-fixed in osmium tetroxide (1% w/v in 0.1M phosphate

buffer), then stained with uranyl acetate (2% w/v in distilled water), dehydrated through increasing concentrations of ethanol (70-100%) and embedded in Spurr resin (Agar Scientific). Semi-thin sections were cut and stained in toluidine blue for specimen orientation. Ultrathin sections (50-80 nm) were prepared using a Reichert Ultracut S Microtome, mounted on 200 mesh nickel grids, and stained lightly with uranyl acetate and lead citrate. Grids were viewed on a JEOL transmission electron microscope (JEM-1010, JEOL, Peabody, MA).

Immunogold labelling

Embryonic and post-natal kidneys were cut in half and immersion fixed in 3% paraformaldehyde in 0.1M phosphate buffer (pH 7.2) at room for 4 hours, transferred to a 10-fold dilution and stored at 4°C. Sections were prepared for immunogold electron microscopy by standard methods[46]. Briefly, segments were stained with uranyl acetate (2% w/v in distilled water), dehydrated through increasing concentrations of methanol (70-100%) and embedded in LR Gold (London Resin Company). Ultrathin sections (50-80nm) were prepared as above, incubated at room temperature for 2 hours with anti-GFP (Rabbit anti-GFP polyclonal Ab, Thermo Fischer Scientific, A11122, 1:1000) and for 1 hour with Protein A-15nm gold complex (British Biocell). All antisera were diluted in 0.1M phosphate buffer containing 0.1% egg albumin. As a control, the primary antibody was replaced by phosphate buffer/egg albumin. After immunolabelling, sections were lightly counterstained with lead citrate and uranyl acetate and were imaged with a JEOL transmission electron microscope as above.

Granule Electron Density Quantification

The mean pixel intensity was determined for each granule and normalized to the cytosol mean pixel intensity. Using this method the darker and more electron-dense the granule, the more negative the normalized mean pixel value.

RNA extraction and quantitative real-time PCR analysis

Total RNA was isolated from frozen tissue using an RNeasy Micro Kit (Qiagen) according to manufacturer's instructions. Kidney was homogenised in RLT buffer by

shaking with a metallic homogenisation bead for 2 min at 30 Hz in a Retsch MM301 tissue disrupter (Haan). Genomic DNA was removed using a DNAFree Kit (Ambion) according to manufacturer's instructions, and the RNA integrity verified using a Nanodrop and gel electrophoresis. cDNA synthesis was carried out using a High Capacity cDNA Reverse Transcription kit (Applied Biosciences) according to manufacturer's instructions.

Mouse renin gene transcription was assessed by quantitative real-time PCR in a volume of 10 µl and monitored on a Roche Lightcycler 480 System using the Universal Probe Library. The primers and probe used for the assays were designed using the Roche Universal Probe Library Assay Design Centre and were obtained from Eurofins Genomic (EU). mRNA levels were normalised to 18S and HPRT mRNA. Mouse renin (UPL probe 16) forward primer: 5'-cccgacatttcctttgacc-3', reverse primer: 5'- tgtgcacagcttgtctctcc-3'; 18S (UPL probe 77) forward primer: 5'-ctcaacacgggaaacctcac-3', reverse primer: 5'-cgctccaccaactaagaacg-3'; HPRT (UPL probe 95) forward primer: 5'-cctcctcagaccgcttttt-3', reverse primer: 5' -aacctggttcatcatcgctaa-3'.

Epifluorescence Microscopy

Imaging

Kidneys were dissected and placed in fresh phenol-free DMEM (10% FBS) on ice until imaging, where they were placed in a petri dish and visualized using a Leica MZ16 F stereomicroscope with top lighting onto a Hammamatsu Orca Flash 4 camera. The light source was a 100 W high-intensity mercury burner lamp, and a standard GFP emission filter was used (470/40nm).

Fluorescence intensity quantification

Images of kidneys were imported into FIJI, any region of interest (ROI) was marked and the mean fluorescence intensity measured. Background mean fluorescence intensity was measured, averaged and subtracted from the mean kidney fluorescence intensity. The area of the ROI was calculated, and the fluorescence intensity normalized to the area. All values are given in arbitrary fluorescence units (A.F.U.).

Kidney renin activity

Kidneys were dissected from male e18 or P1 pups (collected from control or captopril-treated mothers; n = >5 per group), pooled, frozen and sent for analysis (Attoquant GmbH, Austria). Kidneys were powdered under liquid nitrogen and homogenized in phosphate-buffered saline (pH 7.4) by sonication. Protein concentration was determined by Bradford protein assay and normalized in all samples. The samples were diluted in an Ang I-stabilizing inhibitor buffer containing recombinant murine angiotensinogen (50 µg/ml). Samples were split in two parts and incubated at 37 °C in presence or absence of the renin inhibitor aliskiren. The incubation was stopped by acidification and the samples were extracted by Solid-Phase-Extraction prior to LC-MS/MS analysis. The difference of the Ang I level (in nmol/L) in both approaches allowed calculation of the renin-inhibitor-sensitive Ang I formation per hour per mg protein [((nmol/L Ang I) / h) / mg protein], which corresponds to the active renin activity in the tissue.

Statistics

Data was analysed by Student t-test with Tukey's post-hoc analysis and the level of significance was set to $P<0.05$. Error bars represent SEM with * $p<0.05$, ** $p<0.01$, *** $p<0.001$, **** $p<0.0001$ by two-way anova in conjunction with appropriate post hoc analysis.

Results:

Freshly isolated RenGFP$^{+/-}$ kidneys were imaged using epifluorescence microscopy to visualise the extent of renin expression in fetuses and pups at E18.5 and P1 with and without captopril treatment of mothers (Fig. 1A). As expected, renin was expressed throughout the vasculature at both time points and expression at P1 appeared more extensive than at E18.5. By calculating the gross fluorescence intensity from the entire kidney, it was possible to show that whilst there was no difference between treatments in E18.5 kidneys, by P1 captopril treatment had significantly increased GFP expression, suggesting that renin expression was more extensive (Fig. 1B). This was verified using quantitative real time PCR (qRT-PCR) for renin, where renin transcription was only significantly increased in newborns from captopril-treated mothers (Fig. 1C).

To determine whether renin expression was indicative of granulation within the renin-expressing cells, we performed electron microscopy ultrastructure analysis of the cells at the glomerular pole (Fig. 2i) and along major arteries (Fig. 2ii). Sparse granulation was seen in control E18.5 kidneys at the glomerular poles and along arteries, but granulation was considerably increased in captopril-treated, E18.5 kidneys (Fig. 2). More extensive granulation was observed at P1 (Fig. 3), both at the glomerular poles (Fig. 3i) and along major arteries (Fig. 3ii).

The glomerular pole is the nominal location of juxtaglomerular cells, therefore granulated cells are necessarily renin-expressing. However, the vasculature only expresses renin during development and this expression pattern changes over time. To validate our method of identifying granulation in renin-expressing cells, we took advantage of the cytoplasmic GFP expression within and renin-expressing cells in the RenGFP$^{+/-}$ mice by performing anti-GFP immunogold staining. To ensure that the immunogold stain is visible, images have been contrast-enhanced, and examples of the immunogold labelling highlighted using red arrows (Fig. 4). Immunogold staining can clearly be seen in the vascular smooth muscle cells (VSMCs) of major arteries under control conditions, but not in the underlying endothelial cells (Fig. 4A). Similarly, GFP^{+} staining is visible in VSMCs after captopril treatment (Fig. 4B).

Having validated our method of identifying renin-expressing cells, the ultrastructure of these cells was interrogated using electron microscopy. Granules within renin-expressing cells from captopril-treated E18.5 embryos appeared more electron dense compared to water-treated controls, while those in P1 samples exhibited a greater range of electron density after captopril treatment (Fig. 5A-B). To quantify this, the mean pixel intensity was determined for each granule and normalized to the background cytosol mean pixel intensity. The darker and more electron-dense the granule, the more negative the normalized mean pixel value. This confirmed the broadly equivalent electron density of granules from untreated E18.5 and P1 renin-expressing cells, however captopril-treated E18.5 renin-expressing cells showed a lower pixel intensity, indicating more electron dense granules. As expected, there was a more pronounced spread of electron densities of granules from captopril-treated P1 renin-expressing cells (Fig. 5C).

Granules at all stages of granulogenesis were seen across all four groups. Of particular interest were protogranules containing paracrystalline material (Fig. 6A-B). These paracrystalline structures, when magnified sufficiently, were shown to contain regular lattices of proteins (dashed black arrows and black boxes; Fig. 6B-C). Often these also contained small vesicles within the membrane (cyan arrowheads). There were numerous instances of paracrystalline regular lattice material apparently lying outwith a granule membrane (Fig. 6C-D), again with pronounced vesicles in close proximity to the crystalline matter. The paracrystalline material was seen at E18.5 only after captopril treatment, and at P1 in both water and captopril-treated pups.

Another striking ultrastructural alteration brought about by maternal captopril treatment was the extent of rough endoplasmic reticulum (RER) dilation (Fig. 7), suggesting an increase in transcription levels within the cell. This was clearly visible at E18.5 compared to the water controls (Fig. 7A, yellow arrowheads) but was particularly prominent at the P1 timepoint where RER in the water control renin-expressing cells closely resembled that at E18.5, however the RER in captopril-treated cells were vastly dilated and took on an electron-lucent appearance (Fig. 7B).

The increase in renin expression and electron dense granules in P1 kidneys from captopril-treated mothers, coupled with the marked increase in RER size, would

319 suggest that the levels of active renin may similarly be increased. To determine
320 whether this was the case, pooled male kidneys from each timepoint (minimum 5 per
321 group taken from mixed litters) were measured for renin activity (Attoquant GmbH).
322 Results (Table 1) clearly show that the increased granulopoiesis seen in captopril-
323 treated kidneys at P1 was not mirrored by a significant increase in renin activity.
324

Discussion:

Previously it has been shown in the rat that granulation of renin lineage cells occurs only occasionally prenatally [36]. Our preliminary studies suggested a complete lack of granulation in the mouse kidney at E16.5 (data not shown). We confirmed in the mouse the presence of renin immunogold-positive staining, together with occasional granulation, at E18.5, both at the glomerular pole region and within the kidney vasculature of control animals, with increasing granularity by P1. Most VSMCs contained few granules compared to adult recruited cells [47], confirming that the kidneys are still maturing after birth, and suggesting that the controlled secretion of active renin is not normally required perinatally. In the adult, pharmacological ACE inhibition up-regulates renin expression and production in recruited VSMCs as part of a feedback loop response. Using late gestation ACE inhibition, we observed an increase in dense core granules at E18.5 compared to controls, leading to a wide variation in granule electron density by P1. Renin transcript levels reflected dilated endoplasmic reticulum after captopril treatment in both E18.5 and P1 pups, but active stored renin did not show a parallel increase.

We used RenGFP transgenic mice to identify whether renin-expressing cells contained granules or not. This reporter strain had previously been shown to faithfully mark renin gene expression in the developing embryo, being detected in adrenals from E13 and kidney vasculature from E14. The reporter was also shown to regress towards JG cells with kidney development and exhibited recruitment of VSMCs on captopril treatment [42]. We used late gestation (E15.5) captopril administration to mothers in this study, because previously in rats, captopril has been shown to decrease implantation numbers per litter and cause adverse effects on neonatal growth and survival[43]. Since captopril clearly crosses the placenta, we wanted to limit any toxicity.

It has been shown that only 12-15% of renin is packaged into granules in the rat around birth [36], the majority of renin presumably being constitutively secreted. The granules induced in mice by captopril treatment at E18.5 appeared to be classic dense core granules. Induction of granules in JG cells at E18.5 and P1 was also observed in preliminary studies following treatment of pregnant females with a 0.03%Na^+, low

358 salt diet (diet administered from E12.5; data not shown), showing that alternative
359 stimulators of renin transcription also induced granulopoiesis. By P1, the granules
360 were quite varied in electron density with increased numbers of low density or clear
361 granules, which may reflect the lack of increased active renin being stored in dense
362 core granules, suggesting that any increased prorenin expression led to constitutive
363 secretion. Variation in granule electron density following renin gene stimulation in
364 adult JG cells was also described when the human renin gene was used to rescue the
365 mouse *Ren1d* knockout.[48]
366
367 Closer inspection of the proto-granules revealed paracrystalline material, often
368 fringed by small vesicles and partially surrounded by membranes. Similar
369 observations have been made on perinatal granules of the rat. [36] The appearance of
370 these small vesicles and 'ambiguous' membranes[36] around the granules in two
371 separate species deserves further investigation, and may inform us about the early
372 production of granules, crystalline lattices (thought to be prorenin arranged in regular
373 arrays) and /or the activation of renin.
374
375 Renin lineage cells express not only renin but also aldose-keto-reductase, Akr1b7,
376 which exhibits the same pattern of restriction to JG cells during late kidney
377 development, and recruitment under physiological challenge[49]. Like renin, *Akr1b7*
378 transcription is regulated by cAMP signaling [50]. Interestingly, Akr1b7 is not co-
379 localised with renin in granules, but is found in the endoplasmic reticulum[50], where
380 excessive dilatation was observed following captopril treatment, in this study and
381 previously[48,51]. Taken together, the ultrastructural observations imply that captopril-
382 induced increase in transcription and granulopoiesis can outstrip correct packaging
383 into dense core granules both perinatally and in adults.
384
385 The central question is whether increasing granulation following captopril treatment
386 of renin-expressing cells in the developing kidney involves the same mechanism as
387 the increasing granulation seen with VSMC recruitment postnatally? Treatment of
388 newborn rats with an angiotensin II type 1 receptor inhibitor, Losartan, for the first 12
389 days post birth was shown to arrest kidney vascular maturation, resulting in a reduced
390 number of thickened afferent arterioles, together with fewer, smaller glomeruli [52].
391 This suggests that the RAS is playing a key role in kidney development. Using

targeted knockout of vascular versus tubular renin, the defects in kidney development were shown to derive entirely from loss of vascular renin expression [53].

A number of key signals have been identified as playing a crucial role in renin lineage cell recruitment, including RBPj [47], CBP and p300 [54] and microRNAs miR330 and miR125b-5p[55]. Conditional knockout of the transcription factor, RBPj, led to a significant decrease in both glomeruli and number of renin cells in the JGA, which was evident by 1 month of age. Following low salt + captopril treatment of adult mice, any recruited cells had very few granules compared to controls [47]. When the histone acetyl transferases, CBP and p300, which are co-activators of the cAMP response element in the renin promotor, were conditionally knocked out [54] it was shown that the loss of renin-expression only became apparent once the kidney was matured at P30. The two microRNAs, miR330 and miR125b-5p, were found to have opposite effects on renin lineage cell recruitment, miR125-5p being down-regulated while miR330 was up-regulated[55]. Conditional deletion of Dicer, the enzyme which produces active microRNAs, again led to severe vascular and glomerular defects in the developing kidney[56]. Taken together, these studies suggest that there are subtle differences between the timings of stimulatory signals controlling renin expression in perinatal renin-expressing cells versus postnatal JG and recruited cells. On top of this, the presence of additional secretory triggers such as sympathetic nerve activity and establishment of the macula densa, contribute to postnatal blood pressure, water and electrolyte homeostasis [57].

In conclusion, our results add credence to the proposition that the response to captopril of renin-expressing cells in the prenatal and perinatal developing kidney is subtly different from that of the adult kidney. Captopril treatment increases granulopoiesis in cells that are already capable of producing prorenin (which is presumably constitutively secreted) but this apparently outstrips the ability of the ER machinery to correctly fill the dense core granules with active renin.

Table 1: Renin activity measured in pooled e18 and newborn male kidney samples

	Renin Activity
	[((nmol/L Ang I)/h)/ mg protein]
E18 Control	1404
E18 + Captopril	1247
P1 Control	2399
P1 + Captopril	2706
ADULT Control	3529

Abbreviations:

S.E.M = standard error on the mean.

A.F.U = Arbitrary fluorescence units.

A.I.U = Arbitrary intensity units

HPRT = Hypoxanthine guanine phosphoribosyl transferase

VSMCs = vascular smooth muscle cells

ECs = Endothelial cells

RER = Rough endoplasmic reticulum

Acknowledgements:

We wish to thank Professors Stewart Fleming and Jörg Peters for contributions to pilot studies and helpful discussions.

Funding:

Work was funded by BHF Centre for Research Excellence (RE/13/3/30183)

Disclosures:

No conflict of interest declared

References:

1. Okwan-Duodu D, Datta V, Shen XZ, Goodridge HS, Bernstein EA, Fuchs S, Liu GY, Bernstein KE. Angiotensin-converting enzyme overexpression in mouse myelomonocytic cells augments resistance to Listeria and methicillin-resistant Staphylococcus aureus. *J Biol Chem*. 2010;285:39051-39060. doi: 10.1074/jbc.M110.163782
2. Belyea BC, Xu F, Pentz ES, Medrano S, Li M, Hu Y, Turner S, Legallo R, Jones CA, Tario JD, et al. Identification of renin progenitors in the mouse bone marrow that give rise to B-cell leukaemia. *Nat Commun*. 2014;5:3273. doi: 10.1038/ncomms4273
3. Schiffrin EL, Touyz RM. Inflammation and vascular hypertrophy induced by angiotensin II: role of NADPH oxidase-derived reactive oxygen species independently of blood pressure elevation? *Arterioscler Thromb Vasc Biol*. 2003;23:707-709.
4. Wassmann S, Stumpf M, Strehlow K, Schmid A, Schieffer B, Bohm M, Nickenig G. Interleukin-6 induces oxidative stress and endothelial dysfunction by overexpression of the angiotensin II type 1 receptor. *Circ Res*. 2004;94:534-541.
5. Sun Y, Zhang J, Zhang JQ, Weber KT. Renin expression at sites of repair in the infarcted rat heart. *J Mol Cell Cardiol*. 2001;33:995-1003.
6. Starke C, Betz H, Hickmann L, Lachmann P, Neubauer B, Kopp JB, Sequeira-Lopez ML, Gomez RA, Hohenstein B, Todorov VT, et al. Renin lineage cells repopulate the glomerular mesangium after injury. *J Am Soc Nephrol*. 2015;26:48-54. doi: 10.1681/ASN.2014030265
7. Hickmann L, Steglich A, Gerlach M, Al-Mekhlafi M, Sradnick J, Lachmann P, Sequeira-Lopez MLS, Gomez RA, Hohenstein B, Hugo C, et al. Persistent and inducible neogenesis repopulates progenitor renin lineage cells in the kidney. *Kidney Int*. 2017;92:1419-1432. doi: 10.1016/j.kint.2017.04.014
8. Pippin JW, Sparks MA, Glenn ST, Buitrago S, Coffman TM, Duffield JS, Gross KW, Shankland SJ. Cells of renin lineage are progenitors of podocytes and parietal epithelial cells in experimental glomerular disease. *Am J Pathol*. 2013;183:542-557. doi: 10.1016/j.ajpath.2013.04.024
9. Eng DG, Kaverina NV, Schneider RRS, Freedman BS, Gross KW, Miner JH, Pippin JW, Shankland SJ. Detection of renin lineage cell transdifferentiation to podocytes in the kidney glomerulus with dual lineage tracing. *Kidney Int*. 2018;93:1240-1246. doi: 10.1016/j.kint.2018.01.014
10. Poisner AM. The human placental renin-angiotensin system. *Front Neuroendocrinol*. 1998;19:232-252.
11. Poulsen K, Jacobsen J. Enzymic reactions of the renin-angiotensin system. In: Robertson JIS, Nicholls MG, eds. *The renin-angiotensin system*. London: Gower medical Publishing; 1993:5.1-5.12.
12. Poulsen K, Vuust J, Lykkegaard S, Nielsen AH, Lund T. Renin is synthesized as a 50,000 dalton single-chain polypeptide in cell-free translation systems. *FEBS Lett*. 1979;98:135-138.

13. Poulsen K, Vuust J, Lund T. Renin precursor from mouse kidney identified by cell-free translation of messenger RNA. *Clin Sci (Lond)*. 1980;59:297-299.
14. Sealey JE, Rubattu S. Prorenin and renin as separate mediators of tissue and circulating systems. *Am J Hypertens*. 1989;2:358-366.
15. Anderson PW, Macaulay L, Do YS, Sherrod A, d'Ablaing G, Koss M, Shinagawa T, Tran B, Montz FJ, Hsueh WA. Extrarenal renin-secreting tumors: insights into hypertension and ovarian renin production. *Medicine (Baltimore)*. 1989;68:257-268.
16. Corvol P, Pinet F, Plouin PF, Bruneval P, Menard J. Renin-secreting tumors. *Endocrinol Metab Clin North Am*. 1994;23:255-270.
17. Catanzaro DF, Mullins JJ, Morris BJ. The biosynthetic pathway of renin in mouse submandibular gland. *J Biol Chem*. 1983;258:7364-7368.
18. Inagami T, Mizuno K, Naruse M, Nakamaru M, Naruse K, Hoffman LH, McKenzie JC. Active and inactive renin in the adrenal. *Am J Hypertens*. 1989;2:311-319.
19. Taugner R, Kim SJ, Murakami K, Waldherr R. The fate of prorenin during granulopoiesis in epithelioid cells. Immunocytochemical experiments with antisera against renin and different portions of the renin prosegment. *Histochemistry*. 1987;86:249-253.
20. Pratt RE, Carleton JE, Richie JP, Heusser C, Dzau VJ. Human renin biosynthesis and secretion in normal and ischemic kidneys. *Proc Natl Acad Sci U S A*. 1987;84:7837-7840. doi: 10.1073/pnas.84.22.7837
21. Friis UG, Jensen BL, Hansen PB, Andreasen D, Skott O. Exocytosis and endocytosis in juxtaglomerular cells. *Acta Physiol Scand*. 2000;168:95-99.
22. Neves FA, Duncan KG, Baxter JD. Cathepsin B is a prorenin processing enzyme. *Hypertension*. 1996;27:514-517. doi: 10.1161/01.hyp.27.3.514
23. Mercure C, Lacombe MJ, Khazaie K, Reudelhuber TL. Cathepsin B is not the processing enzyme for mouse prorenin. *Am J Physiol Regul Integr Comp Physiol*. 2010;298:R1212-1216. doi: 10.1152/ajpregu.00830.2009
24. Gross KW, Gomez RA, Sigmund CD. Twists and turns in the search for the elusive renin processing enzyme: focus on "Cathepsin B is not the processing enzyme for mouse prorenin". *Am J Physiol Regul Integr Comp Physiol*. 2010;298:R1209-1211. doi: 10.1152/ajpregu.00188.2010
25. Almeida PC, Oliveira V, Chagas JR, Meldal M, Juliano MA, Juliano L. Hydrolysis by cathepsin B of fluorescent peptides derived from human prorenin. *Hypertension*. 2000;35:1278-1283. doi: 10.1161/01.hyp.35.6.1278
26. Hackenthal E, Metz R, Buhrle CP, Taugner R. Intrarenal and intracellular distribution of renin and angiotensin. *Kidney Int Suppl*. 1987;20:S4-17.
27. Stefańska A, Stefańska AM, Péault B, Mullins JJ. Renal pericytes: multifunctional cells of the kidneys. *Pflugers Arch*. 2013;465:767-773. doi: 10.1007/s00424-013-1263-7
28. Stefanska A, Kenyon C, Christian HC, Buckley C, Shaw I, Mullins JJ, Péault B. Human kidney pericytes produce renin. *Kidney Int*. 2016;90:1251-1261. doi: 10.1016/j.kint.2016.07.035
29. Gomez RA, Chevalier RL, Everett AD, Elwood JP, Peach MJ, Lynch KR, Carey RM. Recruitment of renin gene-expressing cells in adult rat kidneys. *Am J Physiol*. 1990;259:F660-665.

30. Gomez RA. Molecular biology of components of the renin-angiotensin system during development. *Pediatr Nephrol*. 1990;4:421-423.
31. Sauter A, Machura K, Neubauer B, Kurtz A, Wagner C. Development of renin expression in the mouse kidney. *Kidney Int*. 2008;73:43-51. doi: 10.1038/sj.ki.5002571
32. Taugner R, Buhrle CP, Hackenthal E, Mannek E, Nobiling R. Morphology of the juxtaglomerular apparatus and secretory mechanisms. *Contrib Nephrol*. 1984;43:76-101.
33. Cantin M, Araujo-Nascimento MD, Benchimol S, Desormeaux Y. Metaplasia of smooth muscle cells into juxtaglomerular cells in the juxtaglomerular apparatus, arteries, and arterioles of the ischemic (endocrine) kidney. An ultrastructural-cytochemical and autoradiographic study. *Am J Pathol*. 1977;87:581-602.
34. Gomez RA, Belyea B, Medrano S, Pentz ES, Sequeira-Lopez ML. Fate and plasticity of renin precursors in development and disease. *Pediatr Nephrol*. 2014;29:721-726. doi: 10.1007/s00467-013-2688-0
35. Sequeira López ML, Pentz ES, Nomasa T, Smithies O, Gomez RA. Renin cells are precursors for multiple cell types that switch to the renin phenotype when homeostasis is threatened. *Dev Cell*. 2004;6:719-728. doi: 10.1016/s1534-5807(04)00134-0
36. Bruhl U, Taugner R, Forssmann WG. Studies on the juxtaglomerular apparatus. I. Perinatal development in the rat. *Cell Tissue Res*. 1974;151:433-456.
37. Egerer G, Taugner R, Tiedemann K. Renin immunohistochemistry in the mesonephros and metanephros of the pig embryo. *Histochemistry*. 1984;81:385-390.
38. Tiedemann K, Egerer G. Vascularization and glomerular ultrastructure in the pig mesonephros. *Cell Tissue Res*. 1984;238:165-175.
39. Minuth M, Hackenthal E, Poulsen K, Rix E, Taugner R. Renin immunocytochemistry of the differentiating juxtaglomerular apparatus. *Anat Embryol (Berl)*. 1981;162:173-181.
40. Ljungvist A, Wagermark J. Renal juxtaglomerular granulation in the human foetus and infant. *Acta Pathol Microbiol Scand*. 1966;67:257-266.
41. Celio MR, Groscurth P, Inagami T. Ontogeny of renin immunoreactive cells in the human kidney. *Anat Embryol (Berl)*. 1985;173:149-155. doi: 10.1007/BF00316297
42. Jones CA, Hurley MI, Black TA, Kane CM, Pan L, Pruitt SC, Gross KW. Expression of a renin/GFP transgene in mouse embryonic, extra-embryonic, and adult tissues. *Physiol Genomics*. 2000;4:75-81. doi: 10.1152/physiolgenomics.2000.4.1.75
43. al-Shabanah OA, al-Harbi MM, alGharably NM, Islam MW. The effect of maternal administration of captopril on fetal development in rat. *Res Commun Chem Pathol Pharmacol*. 1991;73:221-230.
44. McFarlane L, Truong V, Palmer JS, Wilhelm D. Novel PCR assay for determining the genetic sex of mice. *Sex Dev*. 2013;7:207-211. doi: 10.1159/000348677
45. Huerta-Ocampo I, Christian HC, Thompson NM, El-Kasti MM, Wells T. The Intermediate lactotroph: a morphologically distinct, ghrelin-responsive

pituitary cell in the dwarf (dw/dw) rat. *Endocrinology*. 2005;146:5012-5023. doi: 10.1210/en.2005-0335

46. Abel MH, Charlton HM, Huhtaniemi I, Pakarinen P, Kumar TR, Christian HC. An investigation into pituitary gonadotrophic hormone synthesis, secretion, subunit gene expression and cell structure in normal and mutant male mice. *J Neuroendocrinol*. 2013;25:863-875. doi: 10.1111/jne.12081

47. Castellanos Rivera RM, Monteagudo MC, Pentz ES, Glenn ST, Gross KW, Carretero O, Sequeira-Lopez ML, Gomez RA. Transcriptional regulator RBP-J regulates the number and plasticity of renin cells. *Physiol Genomics*. 2011;43:1021-1028. doi: 10.1152/physiolgenomics.00061.2011

48. Buckley C, Nelson RJ, Mullins LJ, Sharp MGF, Fleming S, Kenyon CJ, Semprini S, Steppan D, Peti-Peterdi J, Kurtz A, et al. Phenotypic dissection of the mouse. *J Biol Chem*. 2018;293:1151-1162. doi: 10.1074/jbc.RA117.000160

49. Brunskill EW, Sequeira-Lopez ML, Pentz ES, Lin E, Yu J, Aronow BJ, Potter SS, Gomez RA. Genes that confer the identity of the renin cell. *J Am Soc Nephrol*. 2011;22:2213-2225. doi: 10.1681/ASN.2011040401

50. Lin EE, Pentz ES, Sequeira-Lopez ML, Gomez RA. Aldo-keto reductase 1b7, a novel marker for renin cells, is regulated by cyclic AMP signaling. *Am J Physiol Regul Integr Comp Physiol*. 2015;309:R576-584. doi: 10.1152/ajpregu.00222.2015

51. Taugner R, Metz R. Development and fate of the secretory granules of juxtaglomerular epithelioid cells. *Cell Tissue Res*. 1986;246:595-606. doi: 10.1007/BF00215202

52. Tufro-McReddie A, Romano LM, Harris JM, Ferder L, Gomez RA. Angiotensin II regulates nephrogenesis and renal vascular development. *Am J Physiol*. 1995;269:F110-115. doi: 10.1152/ajprenal.1995.269.1.F110

53. Sequeira-Lopez ML, Nagalakshmi VK, Li M, Sigmund CD, Gomez RA. Vascular versus tubular renin: role in kidney development. *Am J Physiol Regul Integr Comp Physiol*. 2015;309:R650-657. doi: 10.1152/ajpregu.00313.2015

54. Pentz ES, Cordaillat M, Carretero OA, Tucker AE, Sequeira Lopez ML, Gomez RA. Histone acetyl transferases CBP and p300 are necessary for maintenance of renin cell identity and transformation of smooth muscle cells to the renin phenotype. *Am J Physiol Heart Circ Physiol*. 2012;302:H2545-2552. doi: 10.1152/ajpheart.00782.2011

55. Medrano S, Monteagudo MC, Sequeira-Lopez ML, Pentz ES, Gomez RA. Two microRNAs, miR-330 and miR-125b-5p, mark the juxtaglomerular cell and balance its smooth muscle phenotype. *Am J Physiol Renal Physiol*. 2012;302:F29-37. doi: 10.1152/ajprenal.00460.2011

56. Sequeira-Lopez ML, Weatherford ET, Borges GR, Monteagudo MC, Pentz ES, Harfe BD, Carretero O, Sigmund CD, Gomez RA. The microRNA-processing enzyme dicer maintains juxtaglomerular cells. *J Am Soc Nephrol*. 2010;21:460-467. doi: 10.1681/ASN.2009090964

57. Nishimura H, Sequeira-Lopez MLS. Phylogeny and ontogeny of the renin-angiotensin system: Current view and perspectives. *Comp Biochem Physiol A Mol Integr Physiol*. 2021;254:110879. doi: 10.1016/j.cbpa.2020.110879

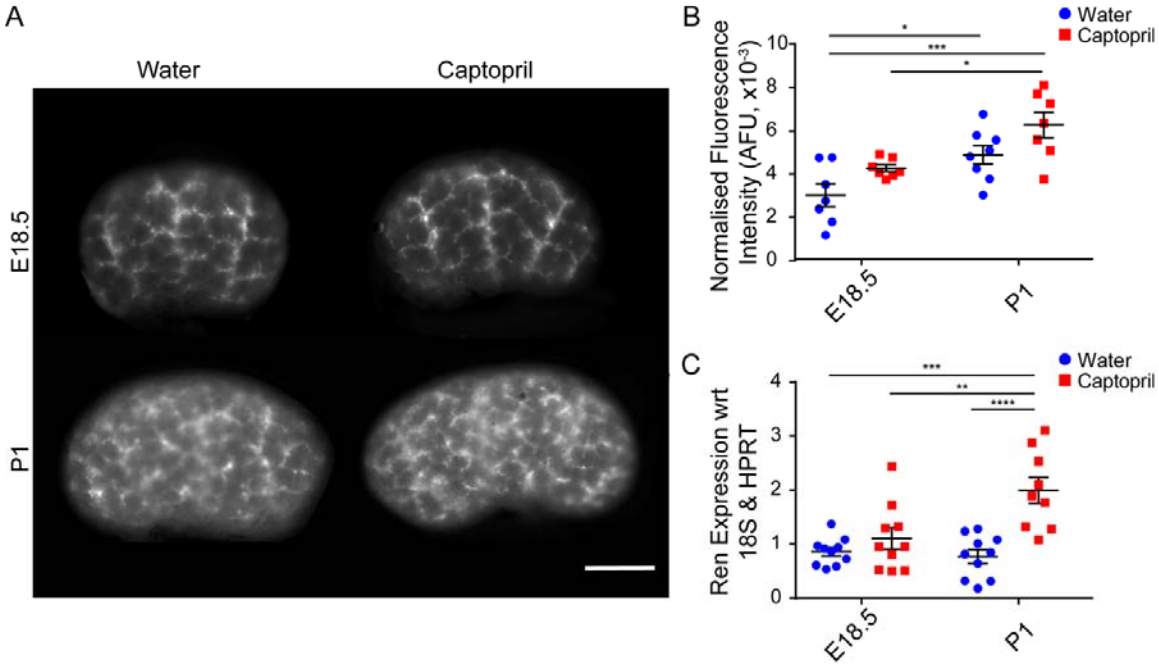

Figure 1 Fetal and post-natal renin expression after maternal water or captopril treatment. **A**. Kidneys from E18.5 and P1 RenGFP$^{+/-}$ mice were dissected and imaged on an epifluorescence microscope to visualize renin expression patterns in controls and after treatment with captopril (30mg/kg/day captopril from E15.5). Scale bars - 0.5mm. **B**. Quantification of mean GFP fluorescence intensity in control (blue; E18.5 n=7, P1 n=8) and captopril-treated (red; E18.5 n=7, P1 n=7) RenGFP$^{+/-}$ kidneys, normalized to the kidney area as imaged using epifluorescence microscopy. **C**. qRT-PCR quantification of renin transcript levels in control (blue; E18.5 n=10, P1 n=10) and captopril-treated (red; E18.5 n=10, P1 n=9) RenGFP$^{+/-}$ kidneys. All error bars represent S.E.M, two way ANOVA with Sidak post hoc test performed for multiple comparisons, **:p<0.01, ***:p<0.001.

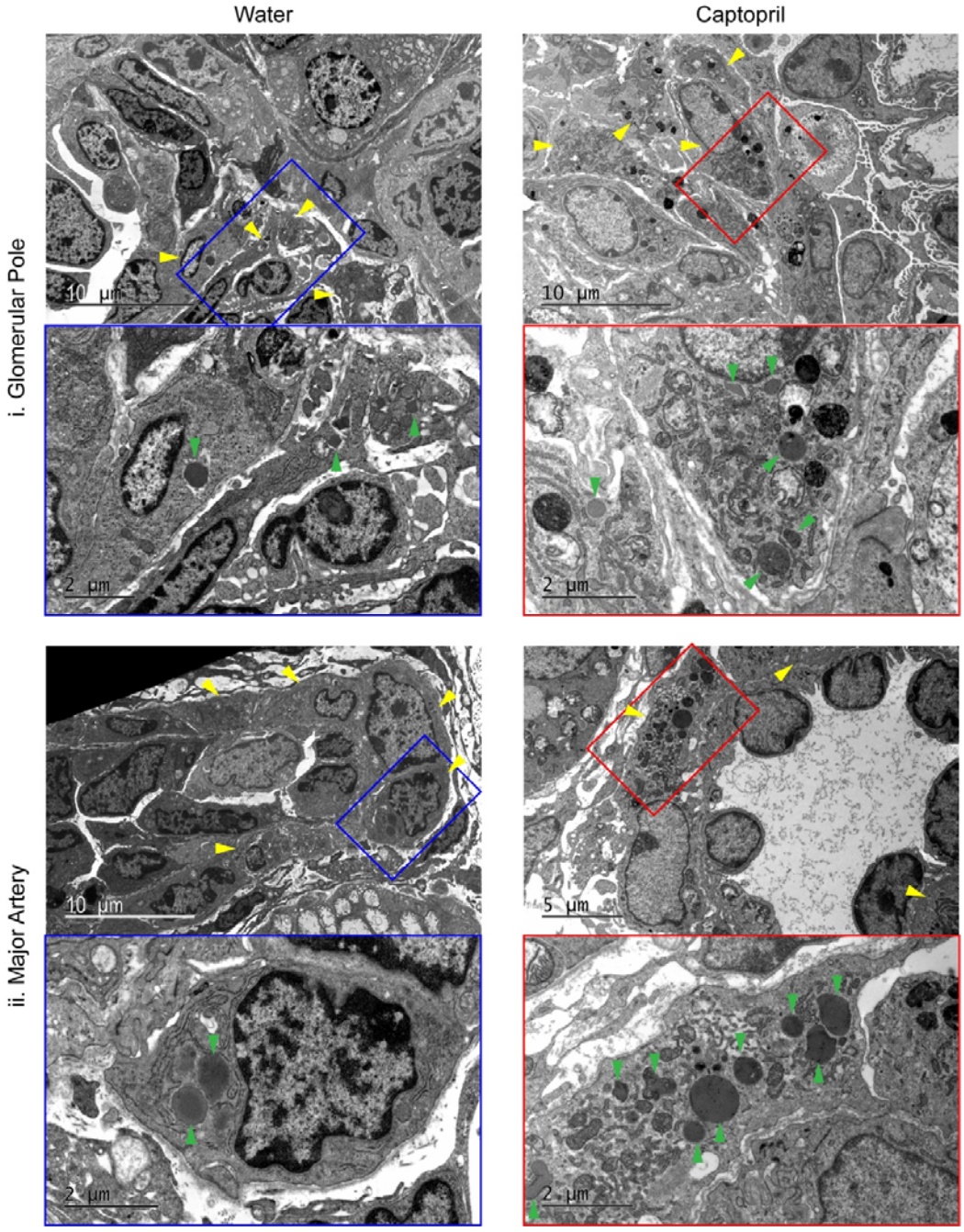

Figure 2: Electron microscopy ultrastructure analysis of E18.5 vasculature after maternal water or captopril treatment. Electron micrographs were taken of control (blue box) and maternal captopril-treated (30mg/kg/day captopril from E15.5) E18.5 embryos (red box) from i. the glomerular pole region and ii. major arteries, showing an overview of the region and a zoomed in renin-expressing cell. Yellow arrows indicate renin-expressing cells; green arrows indicate dense core granules. Scale bars represented individually.

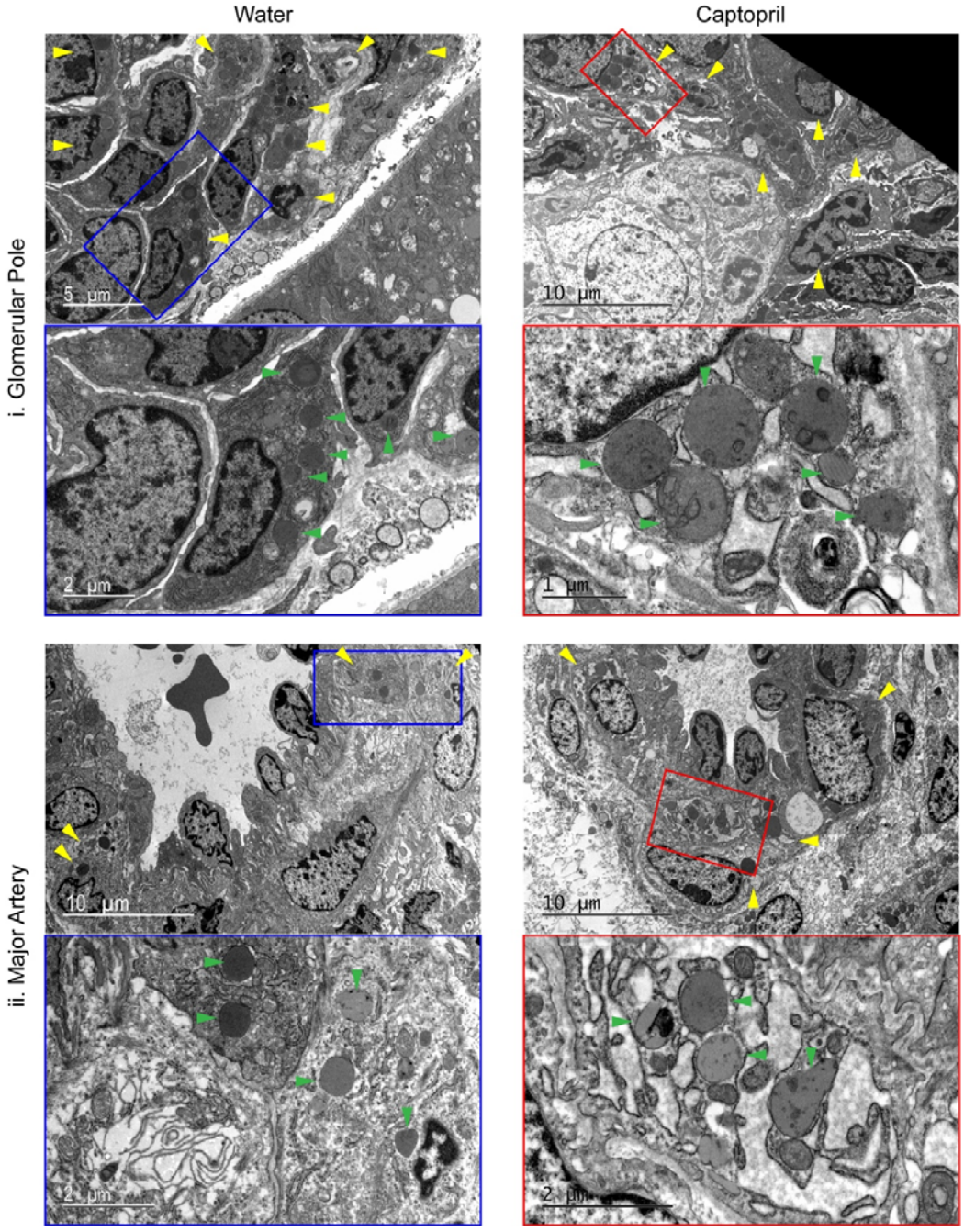

Figure 3: Electron microscopy ultrastructure analysis of P1 vasculature after maternal water or captopril treatment. Electron micrographs were taken of control (blue box) and maternal captopril-treated (30mg/kg/day captopril from E15.5) from i. the glomerular pole region and ii. major arteries, showing an overview of the region and a zoomed in renin-expressing cell. Yellow arrows indicate renin-expressing cells; green arrows indicate dense core granules. Scale bars represented individually.

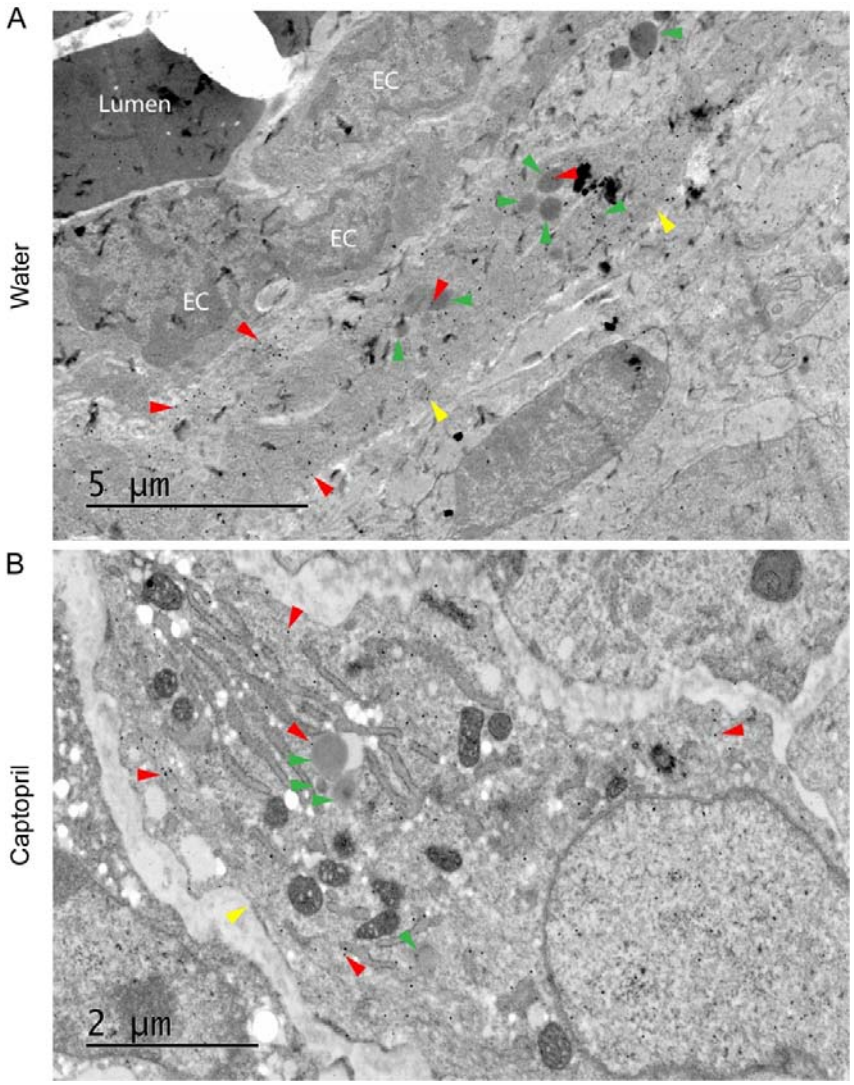

Figure 4: Electron microscopy of immunogold-labelled GFP verifies the presence of GFP-positive renin-expressing smooth muscle cells with granules. Electron micrographs were taken at E18.5 from **A**. control and **B**. maternal captopril-treated (30mg/kg/day captopril from E15.5) kidneys. Lumen = artery lumen; EC = Endothelial cell; Yellow arrows indicate renin-expressing cells; green arrows indicate dense core granules; red arrows indicate immunogold labelling examples. Scale bars represented individually.

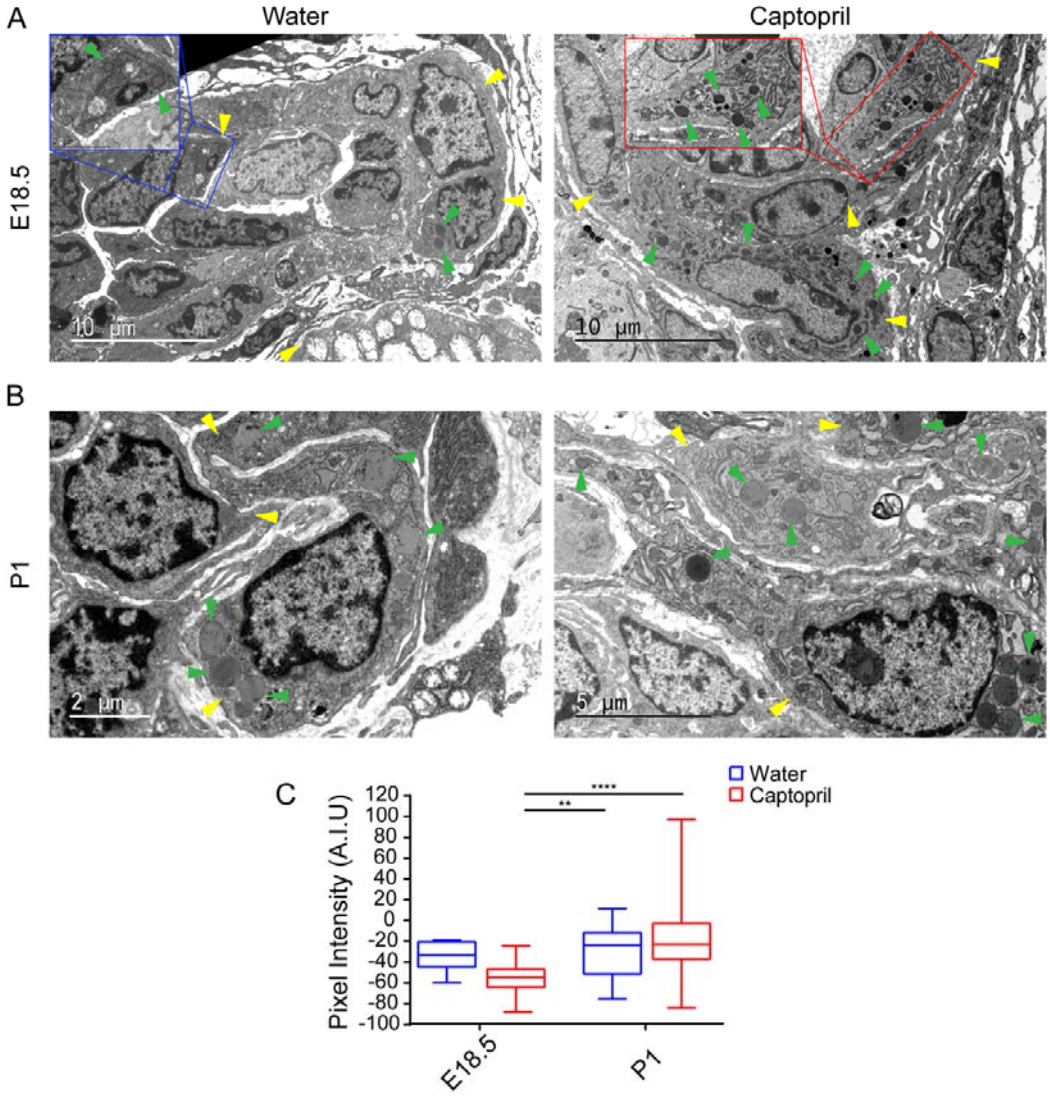

Figure 5: Electron microscopy of cellular ultrastructure reveals differences in granule electron densities between groups. Electron micrographs were prepared from **A**. E18.5 and **B**. P1 kidneys, of control (blue box) and after maternal captopril-treatment (30mg/kg/day captopril from E15.5; red box). **C**. Analysis of granule electron densities, where negative granules indicate a higher electron density. A.I.U = arbitrary intensity unity. Green arrowhead = dense core granule; yellow arrowhead = renin-expressing cell. Scale bars represented individually. Error bars represent outlier values in box and whisker plot, two way ANOVA with Sidak post hoc test performed for multiple comparisons, **:$p<0.01$, ***:$p<0.0001$.

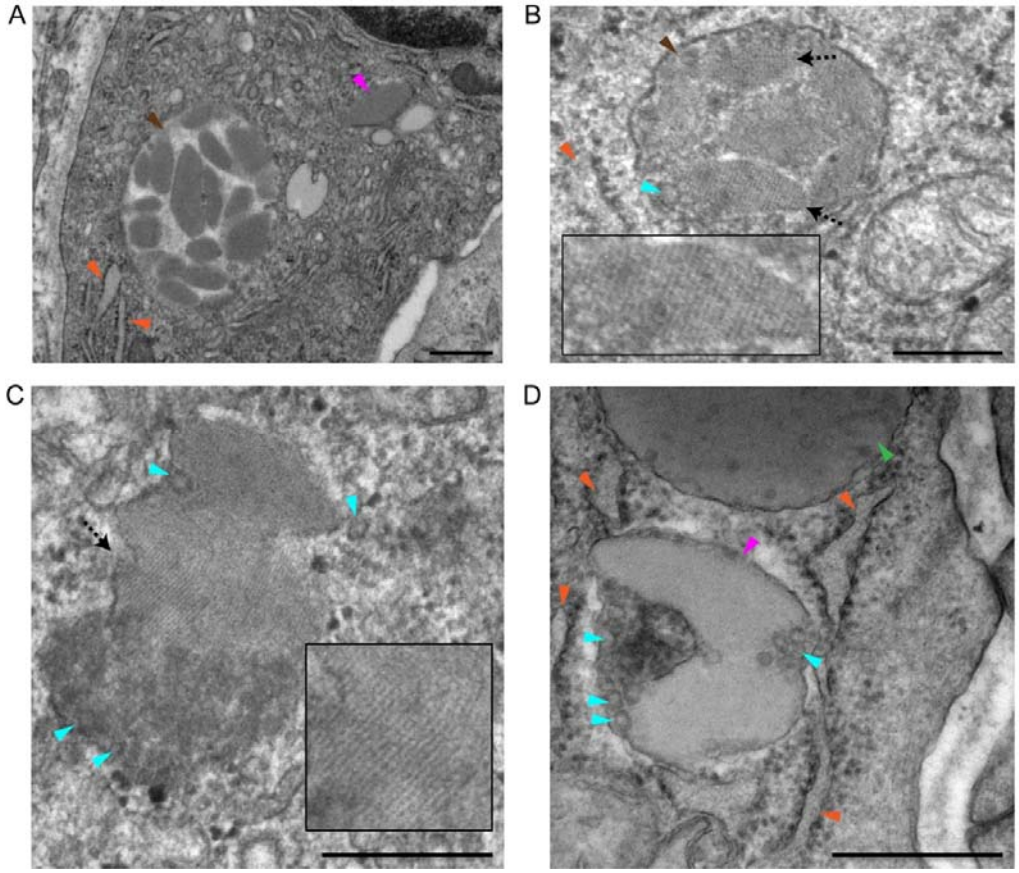

Figure 6: Electron microscopy of granular ultrastructure within renin-expressing cells. **A-B.** Electron micrographs of paracrystalline material accumulating within a granule-like membrane. **C – D.** Electron micrographs of paracrystalline material out-with an obvious granule membrane, with small vesicles closely located. Green arrowhead = granule; Cyan arrowhead = vesicle; orange arrowhead = endoplasmic reticulum; pink arrowhead = paracrystalline material out-with granule membrane; dashed arrow = paracrystalline material lies perpendicular to paracrystalline lattice; brown arrow = paracrystalline structures within membranes. Scale bars - 0.5 μm.

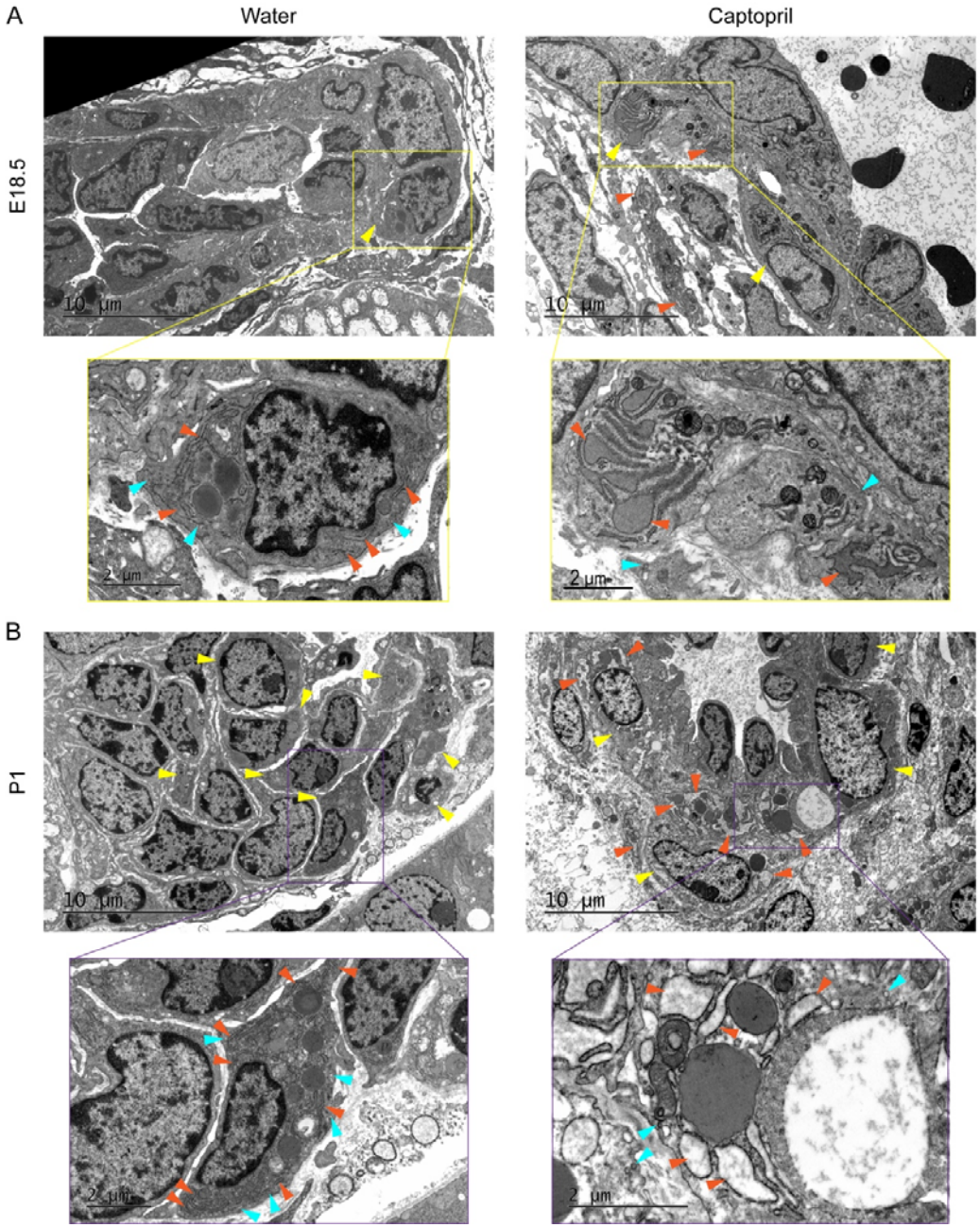

Figure 7: Electron microscopy of cellular ultrastructure reveals dilation of smooth muscle ER after captopril treatment. Electron micrographs were taken from **A**. E18.5 and **B**. P1 under control (water) and after maternal captopril-treated (30mg/kg/day captopril from E15.5) conditions. Yellow arrowhead = renin-expressing cell; cyan arrowhead = vesicle; orange arrowhead = endoplasmic reticulum. Scale bars represented individually.